



Modulation of optical and electrical properties of sputtering-derived amorphous InGaZnO thin films by oxygen partial pressure



X.F. Chen^a, G. He^{a,*}, M. Liu^{b,*}, J.W. Zhang^a, B. Deng^a, P.H. Wang^a, M. Zhang^a, J.G. Lv^c, Z.Q. Sun^a

^a School of Physics and Materials Science, Radiation Detection Materials & Devices Lab, Anhui University, Hefei 230601, PR China

^b Key Laboratory of Materials Physics, Anhui Key Laboratory of Nanomaterials and Nanostructure, Institute of Solid State Physics, Chinese Academy of Sciences, Hefei 230031, PR China

^c Department of Physics and Electronic Engineering, Hefei Normal University, Hefei 230061, PR China

ARTICLE INFO

Article history:

Received 30 April 2014

Received in revised form 22 June 2014

Accepted 29 June 2014

Available online 7 July 2014

Keywords:

Amorphous InGaZnO films

Band gap

Resistivity

Sputtering

ABSTRACT

Sputtering-derived amorphous InGaZnO (a-IGZO) thin films were grown on Si and glass substrates in a mixed ambient of Ar and O₂ at fixed 0.5 Pa working pressure. The influence of O₂/Ar flow ratio on the optical and electrical properties of a-IGZO thin films has been systematically investigated by means of characterization from spectroscopic ellipsometry (SE), X-ray diffraction (XRD), scan electron microscopy (SEM), atomic force microscope (AFM), UV–vis spectroscopy, and electrical measurements. Results have shown that the band gap of the as-deposited IGZO films increases from 3.45 eV to 3.75 eV as the O₂/Ar flow ratio increases from 0% to 20%. Blue shift in band gap and reduction in reactive index with increasing the O₂/Ar flow ratio have been detected. Electrical measurements have indicated the increase in resistivity at higher O₂/Ar gas flow ratio. Related mechanics about the increase in band gap and resistivity have been discussed in detail.

© 2014 Elsevier B.V. All rights reserved.

1. Introduction

Electronic devices with high performance such as microprocessors and power transistors made from crystalline materials have become an important part of the high-technology society in recent years. Si-based thin-film transistors (TFTs) have been widely used as active matrix devices to drive liquid crystal displays (LCDs) [1,2]. Although the mobility of poly-silicon may be higher than 100 cm² V⁻¹ s⁻¹, its processing temperatures are high and it will escalate the cost of TFT production [3]. The mobility of amorphous silicon can be less than 1 cm² V⁻¹ s⁻¹ which limits the transistor's performance [2,4]. Recently, transparent amorphous oxide semiconductors (TAOSs) have been studied extensively for channel materials of thin-film transistors [5]. Advances in oxide semiconductors have shown that the mobility of TFTs based on amorphous structure can reach 10 cm² V⁻¹ s⁻¹ as good as the crystal structure [6,7]. InGaZnO₄ (IGZO) is a kind of transparent and amorphous oxide semiconductor which is made of ZnO [8], doped with In₂O₃ and Ga₂O₃ [9–11]. IGZO thin films are expected to become active layer materials of TFTs for the next generation display technology due to its good electrical properties, high mobility in low-temperature process, sedimentary characteristics and optical properties,

which are important requirements for flat-panel display applications [1,10,12,13].

Based on some publications, it can be noted that it is important to alter the band gap during the deposition process for device application. Based on a patent of US (7550755 B2), it can be noted that the resulting band gap variation of the semiconducting material can be utilized to tune the color of the light emitted from e.g. an LED or a laser. The band gap of the films is generally affected by preparation conditions such as deposition methods, working pressure, substrate temperature, types of substrate, film thickness and O₂/Ar flow ratio. Among them, O₂/Ar flow ratio is one of the most significant parameters to affects film's structure and tune the optical band gap. Thakur et al. [14] have reported the influence of O₂/Ar flow ratio on the performance and stability of Hf–In–Zn–O (HIZO) films. Their results indicated that the band gap and resistivity of HIZO thin films increased with the increase of the O₂/Ar flow ratio from 5% to 50%, which can be attributed to oxygen-incorporation-induced reduction of oxygen vacancies. However, there is still incomplete understanding of the detailed tuning of the band gap with O₂/Ar flow ratio for IGZO films. In order to clarify the effect of the O₂/Ar flow ratio on the optical properties of IGZO thin films, here we present unreported engineering of optical band gap in IGZO thin films with O₂/Ar flow ratio. The sheet resistivity and optical band gap variation of IGZO thin films with O₂/Ar flow ratio from 0% to 20% have been investigated in detail. The influence of O₂/Ar flow ratio on the electrical properties of a-IGZO thin films

* Corresponding authors.

E-mail addresses: hegang@ahu.edu.cn (G. He), mliu@issp.ac.cn (M. Liu).

Table 1
Sputtering rate of IGZO films deposited at various O₂/Ar flow ratio.

O ₂ :Ar flow rate	Thickness of IGZO films (nm)	Deposition rate (nm/min)
0:30	119.22	3.974
1:30	50.22	1.674
2:30	49.89	1.663
3:30	44.74	1.481
6:30	42.81	1.427

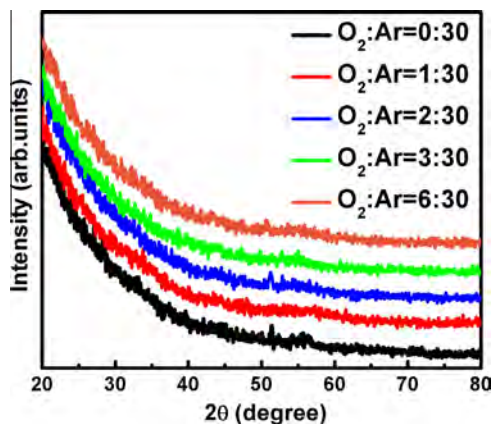


Fig. 1. XRD patterns of IGZO films deposited at various O₂/Ar flow ratio.

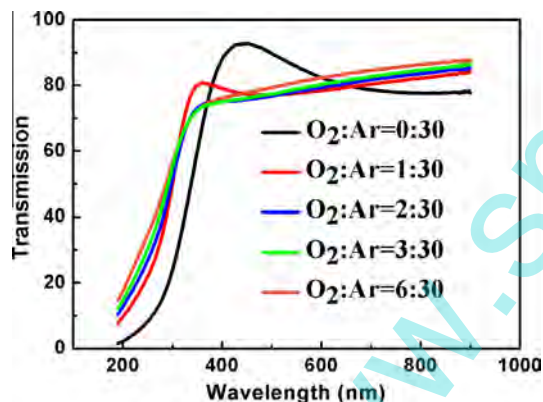


Fig. 2. Transmittance spectra of the IGZO thin films deposited at different O₂/Ar flow ratio.

has also been paid more attention in current work. Additionally, combined with spectroscopic ellipsometer (SE) and UV–vis spectrophotometer, the evolution of the optical band gap related with the O₂/Ar flow ratio has been determined accurately for the first time. Both methods can reduce or avoid the existence of the difference of the optical constant due to the unreasonable fitting model. Previously, little work has been focused on the investigation of the optical band gap as a function of O₂/Ar flow ratio by using SE and UV–vis. Based on our analysis, it can be concluded that the results obtained by Cauchy–Urbach model fitting in SE measurement were consistent with UV–vis spectrophotometer method, indicating the Cauchy–Urbach model fitting in SE measurement is reliable.

2. Experimental details

IGZO thin films were grown on p-type Si (100) wafers with a resistivity of 2–5 Ω cm and quartz substrates by RF sputtering at room temperature using a single ceramic target (the composition of the target is In:Ga:Zn:O = 1:1:1:4). The quartz substrates were only used to investigate the optical properties of IGZO thin

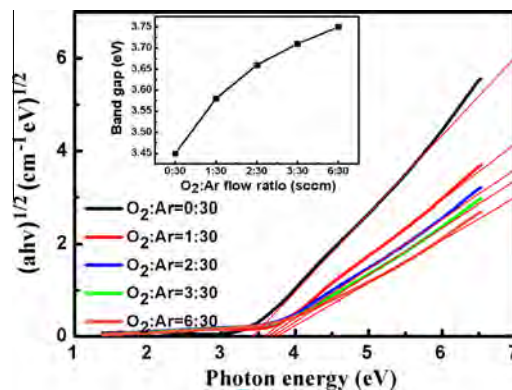


Fig. 3. The optical energy band gap (E_g) of the IGZO films deposited at various O₂/Ar flow ratio.

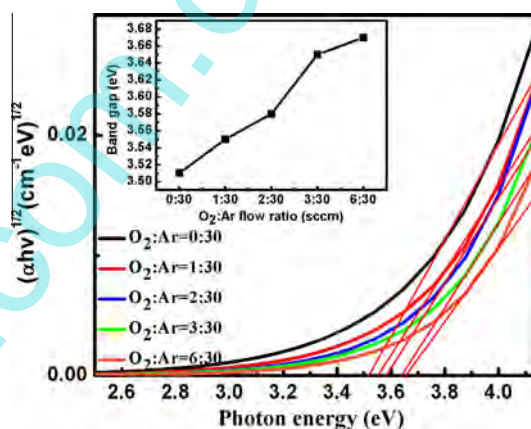


Fig. 4. Plot of $(\alpha hv)^{1/2}$ vs. $h\nu$ for IGZO films deposited at various O₂/Ar flow ratio. The inset shows the optical energy band gap (E_g) of the IGZO films obtained from spectroscopic ellipsometry (SE) deposited at various O₂/Ar flow ratio.

films. Before deposition, the substrates were cleaned using an ultrasonic cleaning in acetone and ethanol for 10 min respectively to remove impurity element, then the substrates were dipped in 1% buffered HF solution to remove any native oxide on the surface. Finally, the substrates were rinsed in deionized water and dried by high purity nitrogen before being placed into the sputtering system. The RF power, deposition pressure, substrate-to-target distance and sputtering time were kept at 40 W, 0.5 Pa, 60 mm, and 30 min, respectively. The flow rate of Ar was constant at 30 sccm, the different flow ratio of O₂/Ar mixture were obtained by changing the flow rate of O₂ to 0, 1, 2, 3, and 6 sccm, respectively. The structural properties of the IGZO films were analyzed by X-ray diffraction (XRD, MXP 18AHF MAC Science, Yokohama, Japan) using Cu K α radiation. The accelerating voltage and current were 40 kV and 100 mA, diffraction angle range from 20° to 80°, 0.02° scanning step and 8°/min scanning speed. The surface morphology of IGZO thin films were determined by scanning electron microscopy (SEM, S-4800). The surface roughness (SR) was checked by ex situ atomic force microscopy (AFM, CSPM4000) in contact mode. The AFM measurements were made with 2 $\mu\text{m} \times 2 \mu\text{m}$ as a scan size, 512 pixels/line. The optical transmission spectra were measured by UV–vis spectrophotometer (Shimadzu, UV-2550) with wavelength ranging from 190 to 900 nm. In addition, the thickness, refractive index, extinction coefficient and dielectric dispersion of the films were examined and fitted by spectroscopic ellipsometer (SC630, SANCO Co., Shanghai) of the rotating analyzer type. The measurements were carried out in air at room temperature in the wavelength range of 280–1100 nm with a step of 10 nm at an incident angle of 65° and 75°. Cauchy–Urbach model [15] was used to obtain the thicknesses and optical constant of the as-prepared IGZO thin films. The resistivity of IGZO films were measured by electrochemical workstation (CHI660D) in ladder wave voltammetry, measuring voltage range from –5 V to 5 V.

3. Results and discussion

The deposition rate of IGZO films deposited at various O₂/Ar flow ratio was shown in Table 1. It can be seen that the deposition rate decreases rapidly from 3.974 to 1.674 nm/min when the O₂

flow rate increases from 0 to 1 sccm, however, with further increasing the O₂ flow rate from 1 to 6 sccm, the deposition rate decreases slightly from 1.674 to 1.427 nm/min. During the sputtering with only Ar, the deposition rate is 3.974 nm/min, which is much higher than that for films deposited with oxygen ambient due to higher mass and impact section of argon ions compared with oxygen [16]. The deposition rate decreases to 1.674 nm/min rapidly when there is oxygen incorporation. This tendency can be explained as following: the development of oxygen partial pressure leads to sputtering atomics' scattering. Moreover, oxygen may diluted argon gas (Argon has stronger sputtering effect than oxygen) and sputtered target atoms collisions intensifier with oxygen atoms in the substrate. Therefore, increasing the oxygen partial pressure also lead to decrease of sputtering rate [17].

Fig. 1 shows the XRD spectra of IGZO films grown at different O₂/Ar flow ratio. No characteristic peaks of In₂O₃, Ga₂O₃, ZnO, and In–Ga–Zn–O are observed, indicating that all the films deposited at room temperature are amorphous independently of O₂/Ar flow ratio. Therefore, it can be inferred that oxygen atoms cannot form crystal structure with Gallium, Indium or Zinc atoms under condition of room temperature.

In order to investigate the optical properties of IGZO films deposited at various O₂/Ar flow ratio, the optical transmission spectra of IGZO films deposited at various O₂/Ar flow ratio are shown in Fig. 2. From the figure, it can be seen that all the IGZO films in ultraviolet wavelengths (200–300 nm) show sharp

absorption edges. During the sputtering with only Ar, the transmission in the visible light range (400–700 nm) is at highest value of 92.76%. The transmission of all the deposited films in the visible light range (400–700 nm) is more than 80%, indicating that the films have very low absorption in the visible and near ultraviolet region. It is higher than any other transparent conductive films [18]. A commercial ITO electrode has a transmittance of about 80% [1], indicating that the deposited films are suitable for display applications. However, the transmittance of the IGZO thin films in visible region reaches to 80% when oxygen is added into the deposition process. This phenomenon may be due to the fact that samples were oxidized after oxygen added into the deposition process.

Fig. 3 shows the optical band gap (E_g) of the IGZO films examined by UV–vis spectroscopy deposited at various O₂/Ar flow ratio. As is known, the E_g of the IGZO films is determined by Tauc relation $(\alpha h\nu)^{1/2} = c(h\nu - E_g)$, where α , $h\nu$, c and E_g are optical absorption coefficient, energy of the incident photon, a constant and optical band gap, respectively [19,20]. Optical band gap energy can be obtained by extrapolating the straight line portion of $(\alpha h\nu)^{1/2}$ against $h\nu$. The intersection of this line with the horizontal axis correspond band gap energy [21]. The value of band gap of the deposited IGZO films is between 3.45 and 3.75 eV. From the figure, the band gap of the deposited IGZO films increases from 3.45 eV to 3.75 eV as the O₂/Ar flow ratio increases from 0% to 20%, which may be explained as the two following reasons: one is the quantum size effect. Some researches indicate that the quantum size

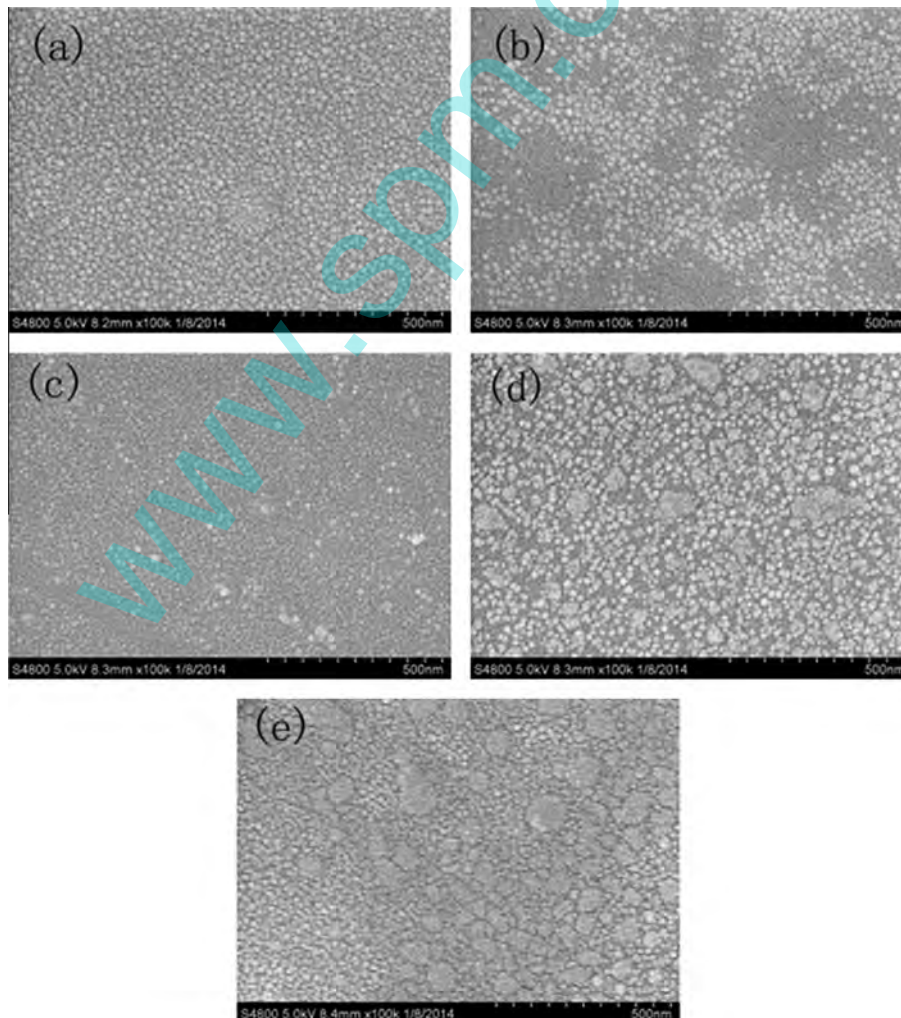


Fig. 5. The SEM images of the IGZO thin films deposited at various O₂/Ar flow ratio. (a) O₂/Ar = 0:30, (b) O₂/Ar = 1:30, (c) O₂/Ar = 2:30, (d) O₂/Ar = 3:30, (e) O₂/Ar = 6:30.

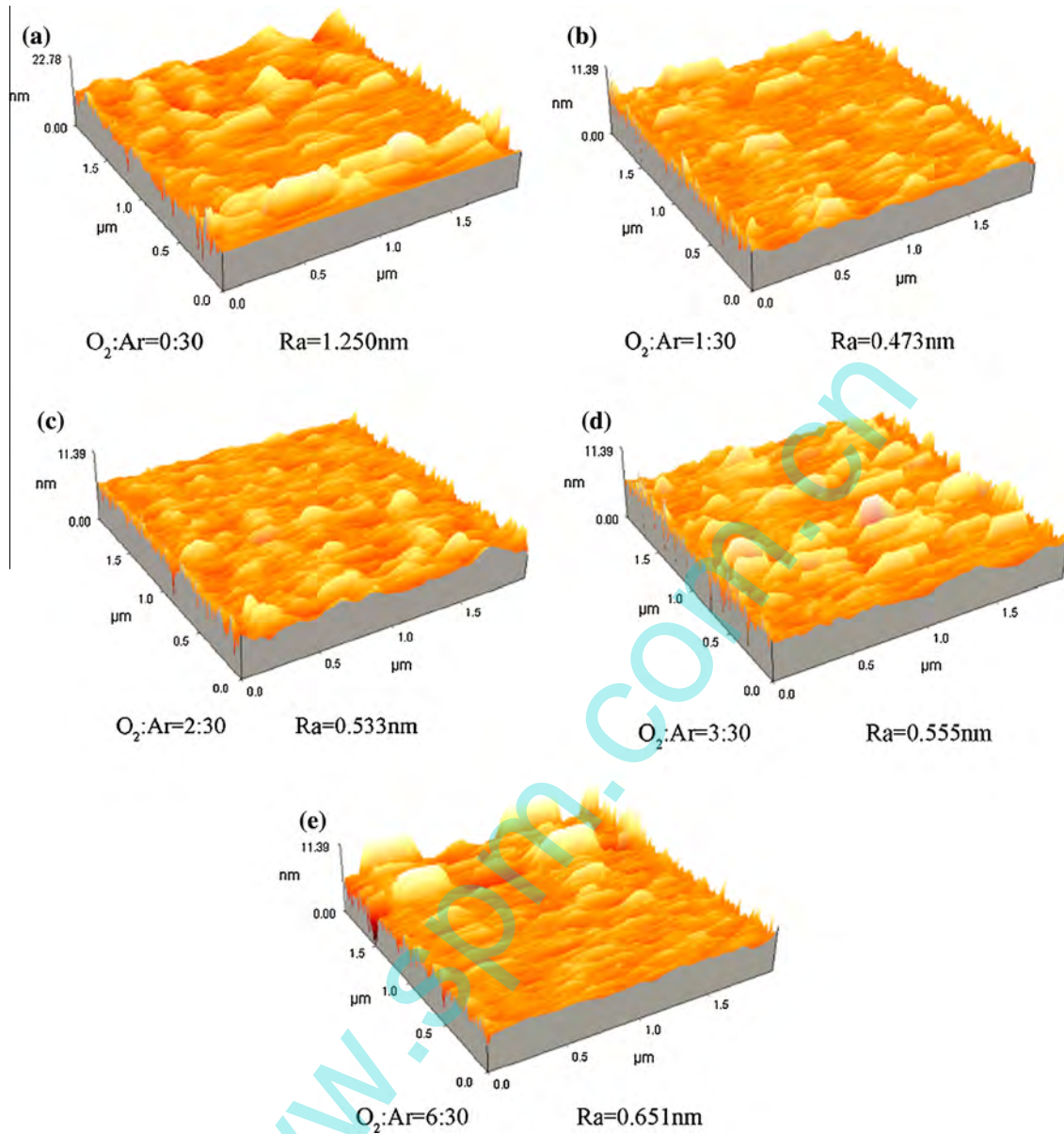


Fig. 6. The AFM images and surface roughness of the IGZO thin films deposited with various O₂/Ar flow ratio.

effect results in a dramatic increase in band gap energy [22]. From SEM, the average grains size of the thin film increase with increasing the O₂/Ar flow ratio, which will decrease the band gap energy of thin films [23]. However, another reason is that the carrier density decreases for oxygen vacancy filled by oxygen atoms with increasing oxygen introducing into the deposition process. The increased oxygen partial pressure makes a-IGZO oxidized and suppresses the oxygen vacancy defects which occupy the bottom of the conduction band [24,25]. So the deduced oxygen vacancy due to high oxidation efficiency will inversely increase the band gap energy of thin films [22].

The absorption coefficient (α) of the samples is calculated via $\alpha(\lambda) = 4\pi k(\lambda)/\lambda$ [26], where k is the extinction coefficient k . The optical band gap (E_g) of the IGZO films can also be determined by Tauc relation as above. The band gaps in the range of 3.51–3.67 eV obtained for the IGZO films are shown in Fig. 4. With the increase of the O₂/Ar flow ratio, the optical band gap (E_g) shifts toward a higher energy, which are similar to the results shown in Fig. 3 obtained from UV–vis spectroscopy.

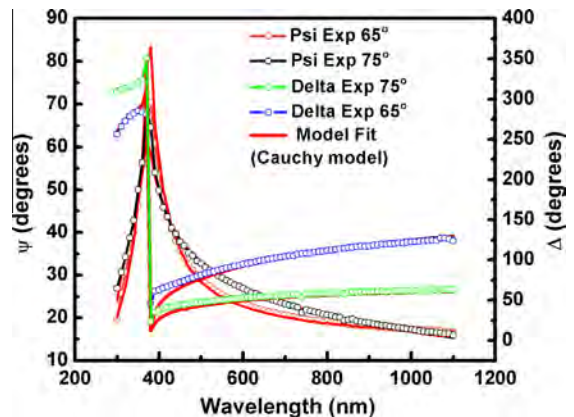


Fig. 7. Experimental (dots) and fitted (solid lines) spectroscopic ellipsometric data of the IGZO film deposited with O₂/Ar flow ratio of 2:30.

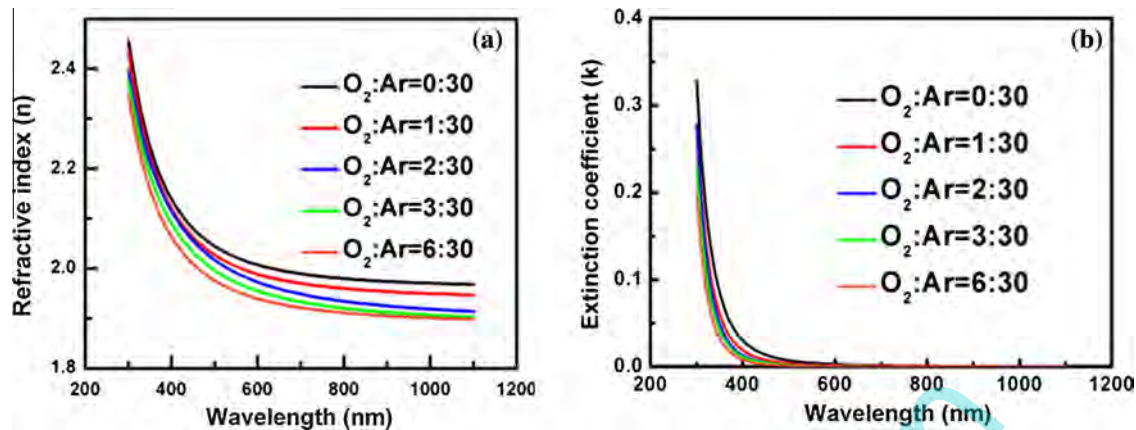


Fig. 8. The refractive index (a) and extinction coefficient k (b) of the IGZO thin films deposited at various O_2/Ar flow ratio.

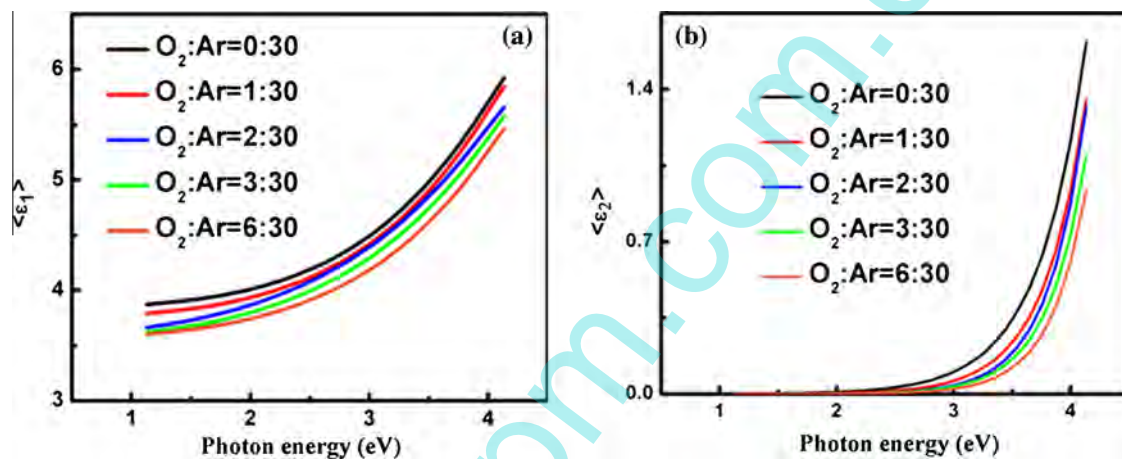


Fig. 9. The real (ϵ_1) and imaginary (ϵ_2) part of dielectric functions of the IGZO films deposited at various O_2/Ar flow ratio.

In order to further confirm the effect of O_2/Ar flow ratio on the surface morphologies and roughness of the IGZO thin films. Figs. 5 and 6 show the SEM and AFM images of IGZO thin films deposited at various O_2/Ar flow ratio, respectively. It can be seen from Fig. 5 that the surface of IGZO film deposited at pure Ar atmosphere is composed of large number of small uniform grains. The sizes of small grains increase unevenly with the increase of the O_2/Ar flow ratio. When O_2/Ar flow ratio is 3:30, irregular grains are observed due to some of the grains were connected into small blocks. Further increasing the O_2/Ar ratio to 6:30, the blocks are more obvious, indicating that with increase of oxygen partial pressure, the density of deposited films decreases. As we know that the sputtered atoms need energy for surface migration. With increasing O_2/Ar flow ratio, the probability of sputtered atoms collides with oxygen atoms increase, which would induce the energy loss become larger. The lower energy would limit the migration of the sputtered atoms on the film surface, leading to form the irregular grains.

Fig. 6 shows the AFM images and surface roughness of IGZO thin films deposited at various O_2/Ar flow ratio. One can see from Fig. 6 that the surface exhibits the most roughness surface with the roughness average (Ra) of 1.25 nm when $InGaZnO_4$ thin film deposited at pure Ar. As we have already showed that the deposition rate is highest at pure Ar, which limits the migration of sputtered atoms, leading to biggest surface roughness of the film. The Ra values are 0.473, 0.533, 0.555 and 0.651 nm for the thin films grown at 1:30, 2:30, 3:30 and 6:30 O_2/Ar flow ratio, respectively. It is considered that when the films deposited at high O_2/Ar ratio,

the collision between the sputtering atoms and oxygen atoms would increase, leading to the decrease of energy of sputtered atoms on the surface, which induce the agglomeration of atoms. As a result, for the IGZO films deposited with O_2 atmosphere, with increasing the O_2/Ar ratio, the observed roughness increase.

The optical properties of the IGZO films were investigated by SE. The Cauchy–Urbach dispersion model was used to fit the data. Among it, the Cauchy expression is expressed as follows: $n(\lambda) = A + B/\lambda^2 + C/\lambda^4$ (A , B and C are the index parameters that specify the index of refraction, relating to the refractive index and the wavelength of light [27]). And the Urbach relationship is $K(\lambda) = a \exp b [12,400/\lambda - 12,400/\gamma]$ (a , b , and γ are the extinction coefficient's amplitude, its described the absorption tail for the sub-band gap absorption at the band gap edge [28]). Three-phase model consisting of IGZO film/ SiO_2 /p-type Si was used to fit the SE date of all IGZO films to obtain their thicknesses and optical constants (the refractive index n and the extinction coefficient k). Experimental (dots) and fitted (solid lines) spectra of IGZO films deposited with O_2/Ar flow ratio of 2:30 at the incident angle of 65° and 75° are shown in Fig. 7. The fit was thus done by minimizing the mean square error (MSE) automatically through a Levenberg–Marquardt algorithm by the ellipsometer's own computer program. It can be seen that in the whole measured energy range the fitted data conform to the experimental data very well, indicating that Cauchy–Urbach model fitting in spectroscopic ellipsometer measurement was reliable and optical properties of the films were described at high precision.

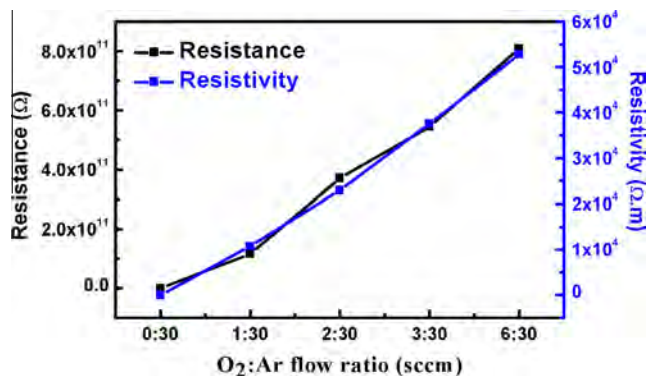


Fig. 10. The resistance and resistivity of IGZO films deposited at various O_2/Ar flow ratio.

Fig. 8(a) and (b) show the fitted refractive index (n) and extinction coefficient (k) of the films deposited at different O_2/Ar flow ratio. The refractive index decreases with the increase of O_2/Ar flow ratio. It's well known that refractive index depend on the density of films [29]. When the films deposited at higher oxygen partial pressure, the collision probability of oxygen atoms and deposited atoms increase, which induce the decrease of the migration energy of deposited atoms, leading to the loose arrangement of the deposited films. Therefore, the refractive index decreases with the increase of the O_2/Ar flow ratio. Fig. 8(b) shows the extinction coefficient k of the films deposited at different O_2/Ar flow ratio. The extinction coefficient decreases with increase of O_2/Ar flow ratio in the range of 300–400 nm, however, it is very low and close to zero in the range of 600–1100 nm, means that the samples have high transmission in this region which is corresponding to the optical transmittance results shown in Fig. 2.

The relationship between refractive index $n(\lambda)$ and dielectric dispersion $\varepsilon(\lambda)$ can be expressed as $n(\lambda) = [\varepsilon(\lambda)]^{1/2} = [\varepsilon_1(\lambda) + i\varepsilon_2(\lambda)]^{1/2}$ [30], the $\varepsilon_1(\lambda)$ and $\varepsilon_2(\lambda)$ are real and imaginary part of $\varepsilon(\lambda)$, which can express as $\varepsilon_1(\lambda) = n(\lambda)^2 + k(\lambda)^2$ and $\varepsilon_2(\lambda) = 2n(\lambda)k(\lambda)$, respectively. The obtained ε_1 and ε_2 of dielectric functions of the IGZO films deposited at different O_2/Ar flow ratio are plotted in Fig. 9. It can be seen that the values of ε_1 and ε_2 are highest when the film deposited at pure Ar condition, and both decrease slightly with the increase of O_2/Ar flow ratio, indicating that O_2/Ar flow ratio has little influence on dielectric properties of IGZO films. The dielectric function of a thin film is closely connected to its microstructure and energy band structure. When a transition from a disordered to a more ordered crystalline phase takes place in a thin film, there is an increase within both real and imaginary part of the dielectric function [31]. No significant changes in ε_1 and ε_2 are observed indicating that there is slight change in microstructure of the samples deposited at O_2/Ar flow ratio. The results are consistent with previous XRD analysis.

To clarify the effect of the O_2/Ar flow ratio on the electrical properties of IGZO thin films, the resistance and resistivity were measured by electrochemical workstation shown in Fig. 10. Table 2 presents the values of the resistance and resistivity of IGZO films.

Table 2

The values of resistance and resistivity of IGZO films.

O_2/Ar flow rate	Resistance (Ω)	Resistivity ($\Omega \cdot m$)
0:30	4.7×10^7	8.55
1:30	1.17×10^{11}	1.07×10^4
2:30	3.70×10^{11}	2.29×10^4
3:30	5.44×10^{11}	3.75×10^4
6:30	8.08×10^{11}	5.28×10^4

The value of resistivity increases from 8.55 to $5.28 \times 10^4 \Omega \cdot m$ when the film deposited at 0:30 to 6:30 O_2/Ar flow ratio, respectively. As is known oxygen vacancies are considered to be the main source of the carriers of IGZO films. With the increase of oxygen partial pressure, oxygen atoms occupied oxygen vacancies increase. The decrease of oxygen vacancies lead to the decrease of carriers, resulting in the increase of resistivity.

4. Conclusions

IGZO thin films were deposited at room temperature with various O_2/Ar flow ratio by RF sputtering. The effect of oxygen partial pressure on the deposition rate, microstructure and optical properties of the IGZO films were evaluated by XRD, SEM, AFM, SE, and UV–vis spectroscopy to clarify. Compared with pure Ar ambient, the deposition rate decreases dramatically under mixture ambient of Ar and O_2 mixture. XRD analysis demonstrates that the sputtering-derived films deposited at room temperature are amorphous in nature. With the increase of the O_2/Ar flow ratio, the band gap and resistivity increases, however, the transmittance and density decrease. Based on analysis, it can be concluded that oxygen-incorporation-induced reduction of oxygen vacancies is suggested to explain the band gap and resistivity increase.

Acknowledgments

The authors acknowledge the support from Anhui Provincial Natural Science Foundation (1208085MF99), National Key Project of Fundamental Research (2013CB632705), National Natural Science Foundation of China (11104269, 51272001), Provincial Natural Science Foundation of Anhui Higher Education Institution of China (KJ2012A023), Key Project of Chinese Ministry of Education (212082), Shanghai Postdoctoral Science Foundation (12R21416800), and Outstanding Young Scientific Foundation of Anhui University (KJQ1103) and “211 project” of Anhui University.

References

- [1] J.L. Wu, H.Y. Lin, B.Y. Su, Y.C. Chen, S.Y. Chu, S.Y. Liu, C.C. Chang, C.J. Wu, *J. Alloys Comp.* 592 (2014) 35–41.
- [2] A. Suresh, P. Gollakota, P. Wellenius, A. Dhawan, J.F. Muth, *Thin Solid Films* 516 (2008) 1326–1329.
- [3] C.C. Lo, T.E. Hsieh, *Ceram. Int.* 38 (2012) 3977–3983.
- [4] J.L. Wu, H.Y. Lin, B.Y. Su, Y.C. Chen, S.Y. Chu, S.Y. Liu, C.C. Chang, C.J. Wu, *Ceram. Int.* 40 (2014) 2419–2425.
- [5] Y.S. Lee, Z.M. Dai, C.I. Lin, H.C. Lin, *Ceram. Int.* 38 (2012) 595–599.
- [6] H. Yabuta, M. Sano, K. Abe, T. Aiba, T. Den, H. Kumomi, K. Nomura, T. Kamiya, H. Hosono, *Appl. Phys. Lett.* 89 (2006) 112123-1–112123-3.
- [7] W. Lim, J.H. Jang, S.H. Kim, D.P. Norton, V. Craciun, *Appl. Phys. Lett.* 93 (2008) 082102-1–082102-3.
- [8] T. Minami, *Semicond. Sci. Technol.* 20 (2005) 35–44.
- [9] E. Fortunato, P. Barquinha, A. Pimentel, A. Goncalves, A. Marques, L. Pereira, R. Martins, *Thin Solid Films* 487 (2005) 205–211.
- [10] K.H. Lee, K.C. Ok, H. Kim, J.S. Park, *Ceram. Int.* 40 (2014) 3215–3220.
- [11] S. Aikawa, P. Darmawan, K. Yanagisawa, T. Nabatame, Y. Abe, K. Tsukagoshi, *Appl. Phys. Lett.* 102 (2013) 102101-1–102101-4.
- [12] S.Y. Huang, T.C. Chang, L.W. Lin, M.C. Yang, M.C. Chen, J.C. Jhu, F.Y. Jian, *Appl. Phys. Lett.* 100 (2012) 222901-1–222901-4.
- [13] H.H. Hsu, C.Y. Chang, C.H. Cheng, S.H. Yu, C.Y. Su, C.Y. Su, *Solid-State Electron.* 89 (2013) 194–197.
- [14] A. Thakur, S.J. Kang, J.Y. Baik, H.B. Yoo, I.J. Lee, H.K. Lee, S.H. Jung, J.H. Park, H.J. Shin, *J. Alloys Comp.* 525 (2012) 172–174.
- [15] J.M. Khoshman, M.E. Kordesch, *Surf. Coat. Technol.* 201 (2006) 3530–3535.
- [16] L. Pereira, P. Barquinha, E. Fortunato, R. Martins, *Mater. Sci. Eng. B* 118 (2005) 210–213.
- [17] M. Cen, Y.G. Zhang, W.L. Chen, P.F. Gu, *Acta Phys. Sin-ch Ed.* 10 (2009) 7025–7028.
- [18] D.S. Ghosh, T.L. Chen, V. Pruneri, *Appl. Phys. Lett.* 96 (2010) 041109-1–041109-3.
- [19] J.I. Pankove, *Optical Processes in Semiconductors*, second ed., Dover Publ., New York, 1975.
- [20] C.F. Klingshirm, *Semiconductor Optics*, Springer, New York, 2005. 797 pp.
- [21] M. Modreanu, J.S. Parramon, O. Durand, B. Served, M. Stchakovsky, C. Eypert, C. Naudin, A. Knowles, F. Bridou, M.F. Ravet, *Appl. Surf. Sci.* 253 (2006) 328–334.

- [22] W.T. Liu, Z.T. Liu, F. Yan, T.T. Tan, H. Tian, *Surf. Coat. Technol.* 205 (2010) 2120–2125.
- [23] S.I. Sadovnikov, A.I. Gusev, *J. Alloys Comp.* 573 (2013) 65–75.
- [24] M. Bender, N. Katsarakis, E. Gagaoudakis, E. Hourdakis, E. Douloufakis, V. Cimalla, G. Kiriakidis, *J. Appl. Phys.* 90 (2001) 5382–5387.
- [25] P.F. Garcia, R.F. Maclean, M.H. Reilly, G. Nunes, *Appl. Phys. Lett.* 82 (2003) 1117–1119.
- [26] L.Q. Zhu, L.D. Zhang, G.H. Li, G. He, M. Liu, *Appl. Phys. Lett.* 88 (2006) 232901-1–232901-3.
- [27] H.H. Güllü, Ö. Bayraklı, I. Candan, E. Coskun, M. Parlak, *J. Alloys Comp.* 566 (2013) 83–89.
- [28] J.M. Khoshman, D.C. Ingram, M.E. Kordesch, *J. Non-Cryst. Solids.* 354 (2008) 2783–2786.
- [29] S.J. Kang, Y.H. Joung, *Appl. Surf. Sci.* 253 (2007) 7330–7335.
- [30] G. He, L.D. Zhang, M. Liu, J.P. Zhang, X.J. Wang, C.M. Zhen, *J. Appl. Phys.* 105 (2009) 014109-1–014109-4.
- [31] G. He, L.Q. Zhu, M. Liu, Q. Fang, L.D. Zhang, *Appl. Surf. Sci.* 253 (2007) 3413–3418.

www.spm.com.cn